

Article

Collective Acceleration of Helium Ions from Its Residual Atmosphere in a Luce Diode

Vladislav Ryzhkov , Mikhail Zhuravlev and Gennady Remnev

National Research Tomsk Polytechnic University, 30, Lenina Ave, 634050 Tomsk, Russia

* Correspondence: ryzhkov@tpu.ru

Abstract: The collective acceleration of helium ions from its residual atmosphere in the Luce diode was studied at helium pressures from 0.13 to 0.23 Pa. The energy of accelerated ions was determined from the drift velocity of the virtual cathode accelerating the ions. The number of ^4He was determined by radioactivities of ^{13}N and ^{30}P induced in h-BN and Al targets via the nuclear reactions $^{10}\text{B}(\alpha, n)^{13}\text{N}$ and $^{27}\text{Al}(\alpha, n)^{30}\text{P}$. The efficiency of capturing ^4He ions in collective acceleration from the residual helium atmosphere was estimated as 0.25%. With increasing helium pressure above 0.15 Pa, the energy of the main ion group noticeably decreased to 0.46 MeV/amu compared to the acceleration from a usual residual atmosphere (~ 0.6 MeV/amu); however, the probability of ion acceleration to a specific energy of up to 1.57 MeV/amu increased significantly. Such increases in the ion energy were accompanied by the appearance of the signal of the second virtual cathode 7–9 ns after the appearance of the first virtual cathode.

Keywords: collective ion acceleration; helium ions; virtual cathode; pulsed ion beam; residual atmosphere



Citation: Ryzhkov, V.; Zhuravlev, M.; Remnev, G. Collective Acceleration of Helium Ions from Its Residual Atmosphere in a Luce Diode. *Quantum Beam Sci.* **2023**, *7*, 33. <https://doi.org/10.3390/qubs7040033>

Academic Editor: Hiroyuki Aoki

Received: 31 July 2023

Revised: 29 August 2023

Accepted: 19 October 2023

Published: 24 October 2023



Copyright: © 2023 by the authors. Licensee MDPI, Basel, Switzerland. This article is an open access article distributed under the terms and conditions of the Creative Commons Attribution (CC BY) license (<https://creativecommons.org/licenses/by/4.0/>).

1. Introduction

The acceleration of helium ions is interesting for the excitation of a number of thermonuclear reactions in astrophysics [1–3] and in an inertial confinement fusion implosion [4], as well as for the production of short-lived radionuclides for radiopharmaceuticals, especially to produce ^{18}F via the reactions $^{16}\text{O}(^3\text{He}, p)^{18}\text{F}$ ($E_{\text{th}} \approx 3.8$ MeV) and $^{16}\text{O}(^3\text{He}, n)^{18}\text{Ne}$ ($Q > 0$) [5,6]. Helium is characterized by the highest single ionization potential, 24.59 eV [7], which reduces the number of its ions in the implementation of collective methods of ion acceleration, for example, by electron rings from the residual atmosphere of the accelerating chamber [8–10]. In [8], an electron ring of $(5\text{--}8) \times 10^{12}$ electrons, accelerated in a falling magnetic field with a gradient of 10 G/cm in a length of 40 cm, was able to capture and accelerate 5×10^9 ions of ^4He to an energy of ~ 30 MeV. A smaller number of electrons in the rings ($\sim 10^{12}$) produced a number of the collectively accelerated ^4He ions of just 10^8 [9]. Up to 10^{10} alpha particles were observed under injecting an intense relativistic electron beam into a decreasing pressure profile of helium gas in a 7 kG external magnetic field [10].

The collective acceleration of helium ions in more compact Plutuo–Luce diodes [11–13] is possible both from the residual gas atmosphere [14,15] and due to synchronized pulsed helium puffing into the near-anode space, as in [10]. It was shown in [14] that the average number of ^{12}C ions captured by the virtual cathode (VC) in acceleration for an h-BN anode insert was 4.8×10^{12} per shot, which, with the expected number of carbon atoms per 15 cm path, is about 2.8×10^{14} , and is translated into the efficiency of capture in the acceleration of ^{12}C ions from the residual atmosphere as 1.7%. When accelerating from the residual atmosphere of deuterium, the number of accelerated deuterons strongly depended on the deuterium pressure in the chamber and, at its pressure of 0.177 Pa, reached an average of 5×10^{11} per shot [15]. Since the number of deuterium atoms at such a pressure on the

path of 9 cm is estimated as 5×10^{14} , the efficiency of the direct capture of deuterons into collective acceleration by the VC on the path of its movement was an order of magnitude less than that of ^{12}C ions—about 0.1%.

Due to the intermediate value of the mass of ^4He ions, it is reasonable to assume that at a close concentration of helium ions in the residual gas, the number of ^4He ions captured by the virtual cathode in the collective acceleration can be higher than the number of deuterons, but lower than the number of carbon ions. On the other hand, taking into account the almost two times higher single ionization potential for ^4He compared to ^2H and ^{12}C , it should be borne in mind that at the same concentrations of ^4He and ^2H atoms in the residual atmosphere, the concentrations of their ions are expected in favor of deuterium ions; therefore, generally speaking, a larger number of ^4He ions captured in the acceleration compared to ^2H is not guaranteed.

During the collective acceleration of ions from the residual helium atmosphere, it is also interesting to determine the effect of this medium on the energy of accelerated ions, since, being three times lighter than ^{12}C ions, ^4He ions create a three-fold lower load on the mover—a VC, which can be expressed in an increase in the probability of the acceleration of ions to much higher energies than are usually observed, since the helium pumped through the chamber can substantially reduce the usual components—hydrocarbons and water vapor—from its residual atmosphere. On the other hand, the peak of ionization losses in helium is significantly shifted towards lower specific ion energy compared to the residual hydrocarbon atmosphere [15]. Therefore, bearing in mind the possibility of the autoregulation of the virtual cathode acceleration due to its achievement of velocities equivalent to the ion energy, at which the peak values of ionization losses are reached [16], it is reasonable to assume that the specific energies of helium ions as a whole can be significantly lower than when accelerating from an ordinary atmosphere. The collective acceleration from the residual helium atmosphere is also of interest for clarifying the contribution of surface contamination of the anode by hydrocarbons and water vapor to the collective acceleration of protons.

Thus, the objectives of this work were to experimentally determine and compare the efficiency of helium ion capture into collective acceleration by a VC in a Luce diode with the efficiency of a deuteron capture, as well as to measure the VC drift velocity to determine the specific energy of collectively accelerated ^4He ions. The peak of ionization losses of ions in helium is shifted to the region of lower energy by 15–20% compared to the losses in the residual atmosphere of air and hydrocarbons; therefore, with the collective acceleration of ions in the residual atmosphere of helium, the specific energy of accelerated ions, under the assumption of a decisive influence on the collective acceleration of ionization losses, is expected to be substantially reduced. To test this assumption, experiments were carried out on the collective acceleration of ^4He ions from its residual atmosphere at a pressure in the range of 0.13–0.23 Pa, combining a radioactivation analysis and Virtual Cathode Time-of-Flight spectrometry (VC-ToF) examined in [17].

2. Materials and Methods

The experimental setup based on a Luce diode mode of accelerator TEMP-4M described in [14,15,17] is shown in Figure 1. Anode inserts with holes of $\text{Ø}12$ mm were made of conventional polyethylene (8 mm thick) and porous Al_2O_3 ceramics (10 mm thick). The end face of a tungsten cathode of $\text{Ø}4$ mm and 20 mm long was flush with the outer side of the anode inserts. Boron nitride (h-BN) plates with sizes of $7 \times 7 \times 0.2$ cm and Al foils with thickness of 100 μm used as targets were placed axially with the cathode and anode at the distance of 25 cm from the latter. To determine the efficiency of capturing helium ions into the collective acceleration, three additional series of 10 shots were taken at a distance of 9 cm from the Al_2O_3 anode to the h-BN targets.

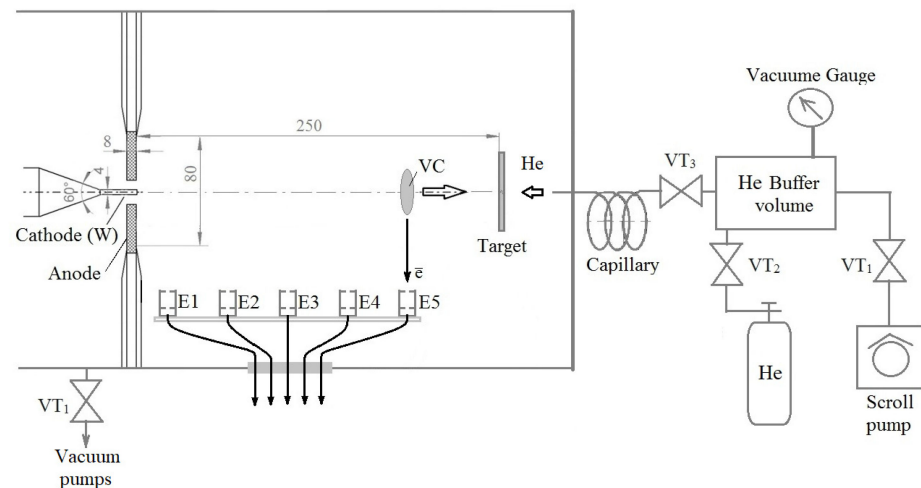


Figure 1. Scheme of the experimental setup: E1–E5 detectors of electrons emitted by virtual cathodes normally to the diode axis; VC—virtual cathode; VT1–VT3—vacuum valves.

Before the whole series of experiments was conducted with the inlet of helium into the working chamber, a 2.5 L He buffer chamber was evacuated with a fore-vacuum scroll pump to a pressure of about 1 Pa through the VT1 valve, after which gaseous helium was let into it through a vacuum valve VT2 to a pressure ranging from 15 to 40 kPa, depending on the required pressure in the working chamber of the accelerator ranging from 0.12 to 0.23 Pa.

By opening the vacuum valve VT3 separating the working chamber of the accelerator and the buffer one, helium was admitted through a 10 m long capillary with an inner channel diameter of 0.6 mm into the working chamber of the accelerator until the required pressure of helium was established in it, the control of which was carried out by an ionization sensor of the PMI-10-2 type, coupled with a controller of the Meradat-VIT19IT2 type. The end of the capillary was placed near the target, while the atmosphere intake of the working chamber by the vacuum pump was located closer to the anode, which could create a helium pressure gradient along the ion acceleration axis in the direction from the target to the anode. In this work, a working chamber of large diameter ($\varnothing 50$ cm) was used; therefore, reliable control of the pressure gradient was not feasible, and thus was not carried out.

After setting the required pressure for 1 min, a series of 10 shots was made for about 60 s, recording the prompt signals for each shot. The time of 60 s was enough for the pressure of the residual atmosphere in the working chamber to not noticeably change for most modes, except for the one performed at the highest pressure (0.23 Pa). On the other hand, ten shots was a large enough number to average the energy and the number of accelerated helium ions in each mode under study. Immediately after a series of shots, the helium pressure in the working chamber was measured again, after which the chamber was opened in order to transfer the irradiated h-BN plate or Al foil to measure the induced activity of ^{13}N (9.965 min) or ^{30}P (2.498 min) with a lead screened Canberra High-Purity Germanium detector. In total, seven series of 10 shots each were carried out at helium pressures of the residual atmosphere of 0.13–0.23 Pa to determine the virtual cathode drift velocity.

Signals from the five VC-ToF electron detectors (E1–E5) as well as signals of the diode voltage and electric current were registered by the digital oscilloscope Tektronix MSO58LP 1 GHz 625 GS/s digital oscilloscope (8 channels). In all the following temporal graphs, the zero point for time is matched at the start of voltage applied to the diode, which was set at about 240 kV by controlling the voltage of the double forming line (Blumlein) [14,15,17]. By measuring current signals of electrons emitted from the virtual cathode normally to the diode axis, the VC-ToF spectrometry described in [17] was used to determine the drift

velocity (and energy) of ions incident on the h-BN plates. The energy of ^4He ions was determined from the speed of the VC and obtained by measuring the VC-ToF signals from the fourth and fifth sensors which were placed at 14.65 and 18.8 cm distances from the anode, respectively.

An average number of ^4He ions in the series n_{He} was determined by the number of ^{13}N and ^{30}P nuclei N_{R} induced in the corresponding h-BN or Al target via the nuclear reactions $^{10}\text{B}(\alpha, n)^{13}\text{N}$ ($Q > 0$, Coulomb barrier $V_{\text{C}} \approx 1.9$ MeV [18]) and $^{27}\text{Al}(\alpha, n)^{30}\text{P}$ ($E_{\text{th}} \approx 3.03$ MeV, $V_{\text{C}} \approx 2.6$ MeV [18]), using a simple equation as follows:

$$n_{\text{He}} = N_{\text{R}}/Y \quad (1)$$

The yields of thick BN or Al(Y) targets, expressed as fractions of ^{13}N or ^{30}P nuclei generated per bombarding the ^4He ion, were borrowed from the energy dependences of the yields of thick reaction targets in [19] (detail please see Supplementary Materials) for each specific energy of the ^4He ion. The number of nuclei N_{R} (^{13}N and ^{30}P) induced in the BN or Al targets, respectively, was determined from the activity of these radionuclides in targets A_{R} (Bq) and normalized to the end of their irradiation, using the following expression:

$$N_{\text{R}} = A_{\text{R}}/\lambda \quad (2)$$

where decay constants of the radionuclides λ (s^{-1}) are defined as $0.6932/T_{1/2}$, while $T_{1/2}(^{13}\text{N}) = 597.9$ s and $T_{1/2}(^{30}\text{P}) = 149.88$ s.

The activities of radionuclides A_{R} are determined from the intensity of the total absorption peaks I_{511} of 511 keV annihilation γ -quanta recorded by a Ge detector with an efficiency $\varepsilon = 0.06$ (6%), according to the following expression:

$$A_{\text{R}} = I_{511}/\varepsilon \cdot f \quad (3)$$

where f is a fraction of 511 keV γ -rays per decay of ^{13}N and ^{30}P ($f = 2$).

The nuclear reaction $^{27}\text{Al}(\alpha, n)^{30}\text{P}$ was used to estimate the fraction of ^4He ions accelerated to energies above 3.034 MeV. It is possible to estimate the fraction of ^4He ions with an energy of more than 6.1 MeV by the threshold nuclear reaction $^{14}\text{N}(\alpha, n)^{17}\text{F}$ ($E_{\text{th}} = 6.088$ MeV) using a target made of a nitride of a medium or heavy element, for example, TiN, when the second element does not create interference when measuring low-level ^{17}F activities ($T_{1/2} = 64.5$ s), while the nuclear reactions $^{10}\text{B}(\alpha, n)^{13}\text{N}$ or $^{27}\text{Al}(\alpha, n)^{30}\text{P}$ produce interfering positron emitters in targets made of boron or aluminum nitrides with more than two orders of magnitude higher yields than the shorter-lived radionuclide ^{17}F , which is produced from Nitrogen [19].

3. Results

3.1. Efficiency of Helium Capture in Collective Acceleration

Measurements of the activity of the ^7Be radionuclide induced by protons via the reaction $^{10}\text{B}(p, \alpha)^7\text{Be}$ in h-BN plates placed at 9 cm distance from Al_2O_3 anodes showed that when helium was admitted into the chamber, the number of protons collectively accelerated per shot was 3–4 times less than during acceleration from the usual residual atmosphere. This indicates a fairly effective “washout” of hydrocarbons and water vapor by helium from the working chamber, even of such a large volume. At a residual helium atmosphere pressure of up to 0.13 Pa, the average number of helium ions per shot for the main group with an energy of 500 keV/amu was 7.9×10^{11} , while the average number of protons was almost two orders of magnitude higher: up to 5×10^{13} with the polyethylene anode inserts. The number of helium atoms on the 9 cm path of a VC (with a cross section of 1 cm^2) to a target at a helium pressure of 0.13 Pa is estimated as 3.18×10^{14} , which translates into the efficiency of the helium captured in collective acceleration as 0.25%. This is 2.5 times higher than the estimate for the efficiency of a capture of deuterons in a collective acceleration from the residual deuterium atmosphere at its pressure of 0.13 Pa—0.1% [15], but 6.8 times lower

than the efficiency for ¹²C ions—1.7% [14]. This result is consistent with the expectations justified in the Section 1.

3.2. Specific Energy of ⁴He Ions in Individual Shots

Table 1 shows the values of the ⁴He ion energy (keV), determined from the VC drift velocity in the seven series of 10 shots in each taken at 25 cm distance from the anode to target. An asterisk indicates higher energy values that were not taken into account in the calculation of the average energy for each series.

Table 1. Energies of ⁴He ions (keV) in the series: vertical columns 1–7 represent different series and horizontal lines 1–10 represent individual shots of the series.

Anode	Polyethylene					Al ₂ O ₃	
p, Pa	0.13	0.14	0.16	0.17	0.2	0.16	0.23
# shots\series	1	2	3	4	5	6	7
1	2952	1708	912	3128	2152	1636	4612 *
2	2792	2152	940	6280 *	1448	1788	3128
3	1708	1568	1508	2260	1288	1240	1288
4	2640	1240	1152	1788	2376	940	4020 *
5	2792	1568	740	2504	6280 *	1448	2376
6	1868	1956	1956	1076	2052	1040	2952
7	2052	1112	1288	1076	2952	2952	1076
8	1956	2640	6280 *	2152	612	1152	940
9	2152	2260	1708	1240	804	2640	2376
10	912	2052	1508	784	1788	2052	2260
Mean E _α , keV *	2182	1826	1301	1779	1719	1689	2050
±S.D. *, keV	628	474	403	789	756	681	845

Below is a line-by-line histogram of the specific energy distribution of ⁴He ions, collectively accelerated in these 7 successive series of 10 shots (according to Table 1), where the numbers give the value of the specific ion energy (keV/amu) for each of these 70 shots, and underlined below are the values for two series made with an Al₂O₃ anode, when the He pressure was 0.16 and 0.23 Pa.

153 185 196 201 228 228 235 235 235
260 269 269 269 278 288 288 310 310 310 322 322 322
362 362 377 377 392 392 409 427 427 427 447 447 447
467 489 489 489 513 513 513 513 538 538 538 538
565 565 565 594 594 594 626
660 660 660 698 698 738 738 738 738
782 782
1005 1153
1570 1570 1570

Of particular note were three cases of acceleration of ⁴He ions with an increased specific energy of 1570 keV/amu or 6.28 MeV as well as two cases with energies of 1005 and 1153 keV/amu or 4.02 and 4.61 MeV, respectively. The same maximum energy of 6.28 MeV coming from the same time-of-flight of 2.4 ns looks more like a limitation for our VC-ToF spectrometer to measure the highest VC/ion velocities. On the whole, it can be observed that the specific energy of the main group of ⁴He ions collectively accelerated from the residual helium atmosphere with a pressure in the range of 0.13–0.23 Pa is indeed significantly shifted compared to the acceleration of protons [14] and deuterons in the normal residual atmosphere [15], when an averaged value of the ion specific energy was about 600 keV/amu. For the main group of ⁴He ions, the average value was 457 ± 175 keV/amu within the range of 153–782 keV/amu for 65 shots (without five shots with the higher energy values). Meanwhile, the average value (for the main group) for two series with the

Al_2O_3 anode insert was close— 470 ± 181 keV/amu within the range of 235–782 keV/amu for 18 shots (without two shots with the higher energy values).

This fact also testifies in favor of the assumption that the composition of the residual atmosphere has a decisive influence on the energy of collectively accelerated ions. On the other hand, with the collective acceleration of ions from the residual helium atmosphere, the probability of the acceleration of ^4He ions to an increased energy (6.28 MeV) noticeably increased. This increase can be attributed, firstly, to the lower load on the virtual cathode from ^{12}C ions “washed out” by helium from the residual atmosphere, and, secondly, due to the possibly increased Ar and Kr impurities in helium compared to the usual residual atmosphere. All cases of acceleration up to an energy of 1153 keV/amu and above were related to a series performed at a helium pressure of at least 0.16 Pa. In any case, it is obvious that the study of the influence of inert gas additions to the residual atmosphere of the working chamber may have prospects for elucidating the features of the collective acceleration of higher-energy groups of ions.

Figure 2 shows the decay curve of ^{30}P activity induced by 10 shots at a helium pressure of 0.13 Pa in an Al target placed at distance of 25 cm from the anode. The number of recorded counts in the peak of annihilation γ -quanta with an energy of 511 keV from ^{30}P during the measurement time $T_{1/2}$ (2.498 min) was determined at the end of irradiation as 32, which provides the number of ^{30}P nuclei induced in the target by ten shots as $32 \times 2/0.06 = 1067$, where 0.06 is the efficiency of the registration of annihilation γ -quanta by the Ge detector. When the $^{27}\text{Al}(\alpha, n)^{30}\text{P}$ reaction yields 10^{-9} at an energy of α -particles of 3.5 MeV [19], this number of ^{30}P nuclei is translated into $\sim 10^{11}$ α -particles per shot.

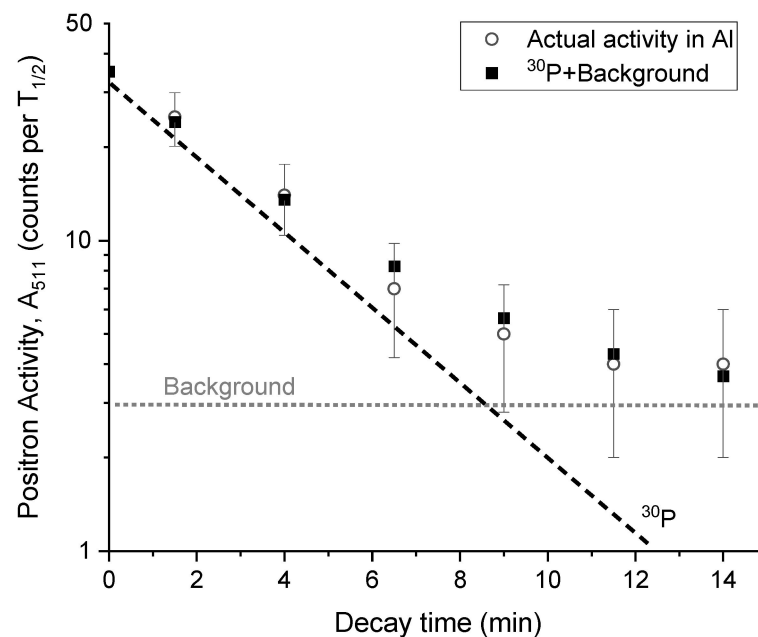


Figure 2. Decay curve of ^{30}P activity induced in Al target.

3.3. Acceleration Dynamics of Helium Ions from Its Residual Atmosphere

Figures 3 and 4 compare VC-ToF signals for the acceleration of ^4He ions to 447 and 1570 keV/amu-specific energies.

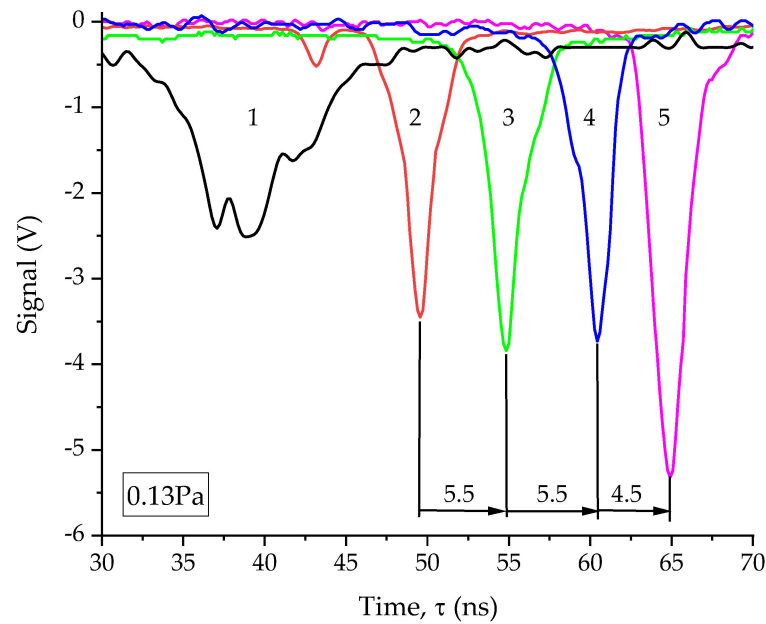


Figure 3. VC-ToF signals for ion acceleration to 447 keV/amu: number 1–5 indicate VC-ToF-signals of E1–E5 detectors, respectively.

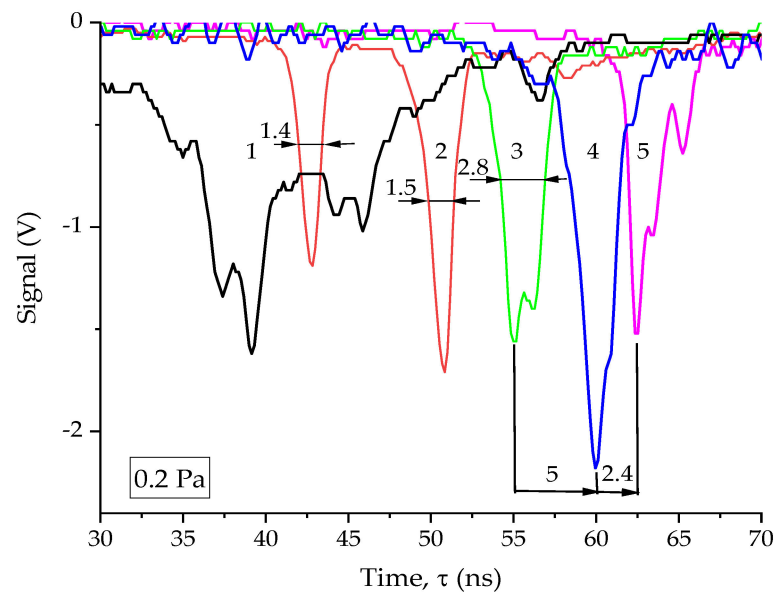


Figure 4. VC-ToF signals for ion acceleration to 1570 keV/amu: number 1–5 indicate VC-ToF-signals of E1–E5 detectors, respectively.

It can be observed that the main difference in the acceleration to a tripled energy is the manifestation in the positions of the first (2.5 cm from the anode) and second VC sensors (6.5 cm from the anode) of three VC signals, of which the first two are comparable in terms of area, and the third, although it looks several times weaker, is clearly distinguished, while in the case of an acceleration to ordinary energy, 447 keV/amu, single VC signals are observed in the positions of the first and second sensors. The possibility of the appearance of a series of up to four consecutive virtual cathodes during the injection of a tubular electron beam (1 MeV) with $\varnothing 8$ cm and a direct current of 9 kA from the side of a narrow section of a monotonically expanding drift conical tube was predicted by modeling in [20]. In our case, the chamber was cylindrical and had a large diameter (50 cm), which suggested the appearance of only one VC. However, pumping helium through the drift space of electron

and ion bunches suggests the existence of a pressure gradient of the residual helium atmosphere along the acceleration axis from the target to the anode, which could contribute to an increase in the probability of the appearance of several VCs during one pulse.

When accelerating to the increased energy (Figure 4), at the positions of the third (10.6 cm from the anode) and fourth (14.65 cm from the anode) VC sensors, the first two VC signals merge into one signal, two times wider than the individual VC signals in position of the second sensor; moreover, this VC signal moves from the position of the third sensor to the fourth one at a speed of approximately 0.88 cm/ns (4.05 cm/4.6 ns), which is equivalent to a specific energy of 400 keV/amu (1.6 MeV). However, in the position of the fifth VC sensor (after 4.15 cm of the way to the target), the VC signal consists of three components, and its first component travels the distance from the fourth to the fifth sensor in 2.4 ns, which is equivalent to a velocity of 1.73 cm/ns and a specific energy of 1570 keV/amu (6.28 MeV). Similar patterns and dynamics of VC signals were typical not only for two other cases of ion acceleration to a specific energy of at least 1570 keV/amu, but also for two cases of ion acceleration to specific energies of 1005 and 1153 keV/amu—see Figure 5.

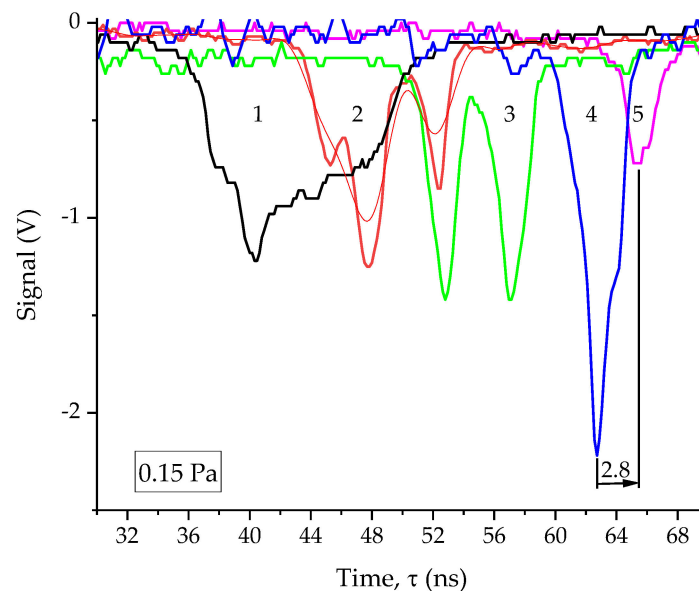


Figure 5. VC-ToF signals for ion acceleration to 1153 keV/amu: number 1–5 indicate VC-ToF-signals of E1–E5 detectors, respectively.

Table 2 presents the interval between the signals BK1 and BK2, which are measured by the detectors E1, E2, E3, E4 and E5. It can be observed that the interval between VK1 and VK2 is reduced to a minimum ($\leq 0.7 \pm 0.3$ ns) at the position of the detector E5, which means that VK2 catches up with VK1 as it approaches the virtual cathode detectors E4 and E5.

Table 2. Parameters of shots with the highest energies of α -particles: $\Delta\tau(i)$ is time between VC1 and VC2 measured by VC(i); $\Delta\tau_{4-5}$ is time-of-flight of VC1 between 4th and 5th VC detectors.

Series-Shot	p, Pa	$\Delta\tau(1)$, ns	$\Delta\tau(2)$, ns	$\Delta\tau(3)$, ns	$\Delta\tau(4)$, ns	$\Delta\tau(5)$, ns	$\Delta\tau_{4-5}$, ns	E_{α} , MeV/amu
#3-8	0.16	4.8	4.5	3.5	2.2	≤ 0.5	2.4	1.57
#4-2	0.17	4.7	4.7	4.7	1.5	≤ 0.5	2.4	1.57
#5-5	0.2	6.7	8	3.2	0.8	0.9	2.4	1.57
#7-1	0.23	5.8	3	3.6	1.2	0.5	2.8	1.153
#7-4	0.23	6	5.2	2.9	1.3	1.2	3	1.005
Mean	0.2	5.6	5.1	3.6	1.4	≤ 0.7	2.6	1.37
\pm S.D.	0.03	0.9	1.9	0.7	0.5	0.3	0.3	0.27

4. Discussion

Compared to the dynamics of a virtual cathode in a conventional residual atmosphere, described in detail in [21] and showing that the VC signals are recorded by the first (E1) and last (E5) detectors for about 25 and 46 ns (after the start of voltage supply to the diode), respectively (see Figure 6 in [21]), in the residual He atmosphere, the VC signals on these detectors appear much later, by 38 and 65 ns (see Figure 3 here). The start time of the acceleration process was defined by the dynamics of the diode current as $\tau_0 \approx 21$ ns [21], which leaves about 4 ns for the VC to move from the anode to the position of the E1 detector (located at a distance of 2.5 cm from the anode) in the usual residual atmosphere, and about 16 ns in the residual atmosphere of He, i.e., 4 times more. Such a delay in the appearance of the VC signal at the first detector (E1) indicates that the time of electron charge neutralization by ions in the residual atmosphere of He is several times longer than in the usual residual atmosphere, and is mainly composed of hydrogen and carbon compounds. This difference is probably due to the highest single ionization potential of ^4He (24.59 eV) compared to all other elements, which is about 2 times higher than the corresponding ionization potentials of ^1H (13.598 eV) and ^{12}C (11.26 eV).

Such a sharp change in the acceleration dynamics of the virtual cathode in the residual helium atmosphere is most likely to be attributed to the fact that the amounts of protons and ^{12}C ions captured in the collective acceleration decrease many times even in the case of using polyethylene anode inserts containing hydrogen and carbon. It was shown in [22] that the number of protons collectively accelerated due to the adsorption and ionization of water vapor and hydrocarbons of the residual atmosphere of the vacuum chamber on the surface of the anode dielectric insert is comparable to the number of protons formed directly from the material of the anode dielectric insert made of polyethylene. The results of this work also indicate that it is the surface contamination of the anode surface, and not the anode material itself, that is the main source of collectively accelerated protons, while the main source for ^{12}C ions is the residual atmosphere itself, as was shown in [14,23]. For this reason, the helium inlet into the working chamber appears to be an effective technique for removing excessive amounts of protons and ^{12}C ions from the residual atmosphere of the working chamber in cases where this is necessary, for example, when accelerating deuterons or α -particles.

Such dynamics of VC-ToF signals during the acceleration of ^4He ions to energies increased by a factor of 2–3 can be explained as follows:

- (1) In some shots, during the passage of electron bunches through the anode hole into the drift space, not one, but two (or even three) VCs are sequentially formed on the outer cut of the anode hole with an interval of 7–9 ns. It should be noted here that at this stage of research there is no certainty that the detected sequences of two or three typical VC signals really represent two or three virtual cathodes corresponding to them, although the possibility of the appearance of a sequence of several VCs was shown for a chamber with increasing diameter [20].
- (2) In such cases, the very first VC (VC1) is electrostatically repulsed by the second VC (VC2) from the anode space before it has time to extract from the near-anode plasma a number of protons comparable to the portion that is usually extracted by single VC, while the VC2 extracts from the near-anode plasma a portion of protons comparable to the usual 5×10^{13} protons, but even with a slightly higher average initial energy, since these protons were already partially drawn from the surface by the VC1 anode.
- (3) Electron bunches oscillating between virtual cathodes and the cathode of the Luce diode and thus accelerating VCs are predominantly reflected from the VC2, which thus shields VC1; therefore, the oscillating electrons only partially transfer the energy to VC1, transferring the energy to a much greater extent to VC2. Thus, VC2 accelerates faster and catches up with VC1, even despite their mutual electrostatic repulsion that accelerates VC1 before it reaches the target if the latter is set at a sufficiently large distance ($Z \geq 10$ cm).

- (4) At the point of mutual approach of these two VCs ($Z \geq 10$ cm), VC1 is the least loaded with protons, which it partially captures from the near-anode plasma (e.g., $\leq 0.5 \times 10^{13}$); with even lower efficiency from the residual atmosphere, both VCs could be loaded nearly equally with ^4He ions ($\leq 2.5 \times 10^{11}$).
- (5) At the point of the closest approach of VC2 and VC1, they mutually repel each other, as a result of which the less inertial VC1 acquires a significant translational momentum, accelerating the ions (including protons) captured by it to an increased energy, and VC2 slows down to the extent determined by the mass ratio ions in these conditional electron-ion bunches.
- (6) With an increase in the distance between these two VCs, the mutual repulsion between them weakens, which, together with a decrease in ionization losses by accelerated ions, leads to a drift of both VCs and ion bunches captured and accelerated by them, while the acceleration and, ultimately, the drift velocity of the leading VC1 and bunch of protons and ^4He ions accelerated by it is determined to the greatest extent by the number of protons accelerated by the second virtual cathode; thus, it is a random variable from shot to shot.

It is reasonable to assume that the number of protons captured in the VC1 acceleration from the near-anode plasma is the smaller, the shorter the pause between VC1 and VC2, while a smaller number of protons are accelerated to a higher energy, which is shown in [15,17,21]. Thus, the acceleration of ^4He ions in the residual helium atmosphere agrees with the data of [21] which showed that the group of high-energy protons is represented by outrunning bunches, while the main group of protons is represented by a retarding bunch. A continuation of the study of the collective acceleration of ^4He ions from the residual helium atmosphere is seen in research of the addition of Ar and Kr s to the pumped helium; it is also worth investigating possible effects in the formation of inert gas gradients in both directions along the ion acceleration axis—from the target to the anode, and vice versa—from the anode to the target. To do this, it is desirable to significantly reduce the diameter of the drift tube and ensure that the pressure of the residual atmosphere is measured both near the target and near the anode hole. Intrinsic magnetic fields of relativistic electron flows affect the formation and dynamics of a virtual cathode [24]; therefore, further development of this research involves measuring the signals of the azimuthal component of such magnetic fields with differential sensors, comparing these signals with the signals of the spectrometer used in this work.

5. Conclusions

The efficiency of capturing ^4He ions in a collective acceleration from the residual helium atmosphere at a pressure of 0.13 Pa in the Luce diode has been estimated as 0.25%, which is noticeably higher than when accelerating deuterons from the residual deuterium atmosphere at the same pressure—0.1% [15], but 6.8 times lower than the efficiency for ^{12}C ions—1.7% [14]. Under acceleration from the residual helium atmosphere, the energy of the main group of ions (0.47 MeV/amu) noticeably decreases compared to acceleration from the usual residual atmosphere, e.g., 0.6 MeV/amu, on average, for 10 series of 10 shots each, and performed at pressures of the usual residual atmosphere in the range of 0.03–0.21 Pa, as calculated from Table 1 in [23]. The same value (0.6 MeV/a.m.u.) was determined in [15] for the acceleration of deuterons from the residual atmosphere of the deuterium at pressures of 0.04 and 0.12 Pa—see Table 2 in [15]. However, the probability of ion acceleration to a specific energy of two to three times higher than that of the main group, up to 1.57 MeV/amu, increases noticeably with the increasing helium pressure above 0.15 Pa. It was found that such an increase in the ion energy is accompanied by the appearance of the signal of the second virtual cathode 7–9 ns after the appearance of the signal of the first virtual cathode. A simple explanation has been proposed for the acceleration of ions to an increased energy with such a rapid appearance of the second virtual cathode.

Supplementary Materials: The following supporting information can be downloaded at: <https://www.mdpi.com/article/10.3390/qubs7040033/s1>, The paper refers on [19] as supplementary files for yields of nuclear reactions $^{10}\text{B}(\alpha,n)^{13}\text{N}$ and $^{27}\text{Al}(\alpha,n)^{30}\text{P}$ taken from Figure 16 and Figure 49, respectively, in the attached paper by Murata et al. [19]. The yield plots in the above Figures were carefully digitized using Origin Pro 2022 Software to determine the reaction yields for each measured alpha particle energy.

Author Contributions: Conceptualization, V.R.; Data curation, V.R.; Formal analysis, V.R.; Funding acquisition, G.R.; Investigation, V.R. and M.Z.; Methodology, V.R. and M.Z.; Project administration, G.R.; Resources, G.R.; Supervision, V.R. and G.R.; Validation, V.R. and M.Z.; Visualization, V.R.; Writing—original draft, V.R.; Writing—review and editing, V.R. All authors have read and agreed to the published version of the manuscript.

Funding: This research was funded by a grant Russian Science Foundation № 23-19-00614, <https://rscf.ru/en/project/23-19-00614/> (accessed on 20 October 2023).

Data Availability Statement: Data will be available on request.

Conflicts of Interest: The authors declare no conflict of interest.

References

1. Liu, Q.; Febraro, M.; deBoer, R.; Aguilar, S.; Boeltzig, A.; Chen, Y.; Couder, M.; Gorres, J.; Weaver, J.; Macon, K.; et al. Low energy cross section measurement of the $^{10}\text{B}(\alpha,n)^{13}\text{N}$ reaction and its impact on neutron production in 1st generation stars. *Phys. Rev. C* **2020**, *101*, 025808. [[CrossRef](#)]
2. Van der Zwan, L.; Geiger, K.W. The $^{10}\text{B}(\alpha,n)^{13}\text{N}$, $^{13}\text{N}^*$ cross section for α -energies from 1.0 to 5 MeV. *Nucl. Phys. A* **1973**, *216*, 188–198. [[CrossRef](#)]
3. Prior, R.M.; Spraker, M.C.; France, R.H.; Stave, S.; Ahmed, M.; Karwowski, H.; Mueller, J.M.; Myers, L.S.; Weller, H.R. The total cross sections of the $^{11}\text{B}(\alpha,n)^{14}\text{N}$ and the $^{10}\text{B}(\alpha,n)^{13}\text{N}$ reactions between 2 and 6 MeV. *Nucl. Sci. Tech.* **2017**, *28*, 106. [[CrossRef](#)]
4. Lonardoni, D.; Sauppe, J.P.; Batha, S.H.; Birge, N.; Bredeweg, T.; Freeman, M.; Geppert-Kleinrath, V.; Gooden, M.E.; Hayes, A.C.; Huang, H.; et al. First measurement of the $^{10}\text{B}(\alpha,n)^{13}\text{N}$ reaction in an inertial confinement fusion implosion at the National Ignition Facility: Initial steps toward the development of a radiochemistry mix diagnostic. *Phys. Plasmas* **2022**, *29*, 052709. [[CrossRef](#)]
5. Bishop, A.; Satyamurthy, N.; Bida, G.; Phelps, M.; Barrio, J.R. Production of $^{18}\text{F}[\text{F}_2]$ using the $^{16}\text{O}(\alpha,n)^{18}\text{F}$ reaction. *Nucl. Med. Biol.* **1996**, *23*, 385–389. [[CrossRef](#)]
6. Sadat, S.K.; Adlparvar, S.; Sheibani, S.; Elahi, M.; Safarian, A.; Farhangi, S.; Dabirzadeh, A.A.; Khalaj, M.M.; Vosoughi, Y.; Moslehi, A.; et al. Production of $^{16}\text{O}(\alpha,n)^{18}\text{F}$ and $^{20}\text{Ne}(d,\alpha)^{18}\text{F}$ Short-Lived Radioisotopes with a Plasma Focus. *J. Fusion Energy* **2011**, *30*, 459–461. [[CrossRef](#)]
7. Kaufman, M.J.; Trowbridge, C.G. The Ionization Energy of Helium. *J. Chem. Educ.* **1999**, *76*, 88. [[CrossRef](#)]
8. Sarantsev, V.P.; Rashevskii, V.P.; Kaminskii, A.K.; Mironov, V.I.; Fartushnyi, V.P.; Sergeev, A.P.; Novikov, V.G.; Tyutyunnikov, S.I.; Kaminskaya, A.M. Experiments on acceleration of a particles by the collective method. *Sov. Phys. JETP* **1971**, *33*, 1067–1069.
9. Schumacher, U.; Andelfinger, C.; Ulrich, M. Collective acceleration of protons and helium ions in the Garching ERA. *IEEE Trans. Nucl. Sci.* **1975**, *22*, 989–991. [[CrossRef](#)]
10. Mako, F.; Fisher, A.; Rostoker, N.; Tzach, D.; Roberson, C.W. Collective Ion Acceleration Controlled by a Gas Gradient. *IEEE Trans. Nucl. Sci.* **1979**, *26*, 4199–4201. [[CrossRef](#)]
11. Belensov, P.E. Comments on the article “Collective acceleration of ions by systems with a virtual cathode”. *Physics-Uspokhi* **2004**, *47*, 209. [[CrossRef](#)]
12. Luce, J.S.; Sahlin, H.; Crites, T.R. Collective acceleration of intense ion beams in vacuum. *IEEE Trans. Nucl. Sci.* **1973**, *20*, 336–340. [[CrossRef](#)]
13. Dubinov, A.E.; Kornilova, I.Y.; Selemir, V.D. Collective ion acceleration in systems with a virtual cathode. *Physics-Uspokhi* **2002**, *45*, 1109–1129. [[CrossRef](#)]
14. Ryzhkov, V.A.; Pyatkov, I.N.; Remnev, G.E. Selective determination of collectively accelerated ^{12}C ion bunches by neutron time-of-flight spectrometry. *Nucl. Instrum. Methods Phys. Res. A* **2022**, *1036*, 166871. [[CrossRef](#)]
15. Ryzhkov, V.A.; Pyatkov, I.N.; Remnev, G.E. Collective acceleration of deuterons from the residual chamber atmosphere in a Luce diode. *Vacuum* **2022**, *202*, 111212. [[CrossRef](#)]
16. Ziegler, J.F.; Ziegler, M.D.; Biersack, J.P. SRIM—The stopping and range of ions in matter (2010). *Nucl. Instrum. Methods Phys. Res. Sect. B* **2010**, *268*, 1818–1823. [[CrossRef](#)]
17. Ryzhkov, V.A.; Pyatkov, I.N.; Remnev, G.E. Control of virtual cathode dynamics under collective acceleration of protons in a Luce diode. *Nucl. Instrum. Methods Phys. Res. A* **2022**, *1042*, 167436. [[CrossRef](#)]
18. Bass, R. *Nuclear Reactions with Heavy Ions*; Springer: Berlin/Heidelberg, Germany, 1980; pp. 326–332.
19. Murata, T.; Matsunobu, H.; Shibata, K. Evaluation of the (a,xn) Reaction Data for JENDL/AN-2005. JAEA-Research 2006-052; 2006. Available online: <https://jopss.jaea.go.jp/pdfdata/JAEA-Research-2006-052.pdf> (accessed on 14 July 2023).

20. Dubinov, A.E.; Tarakanov, V.P. Simulated Formation of a Virtual Cathode Chain in a Conical Drift Tube. *Tech. Phys. Lett.* **2019**, *45*, 754–756. [[CrossRef](#)]
21. Ryzhkov, V.A.; Pyatkov, I.N.; Remnev, G.E. Time-resolved γ -spectrometer to promptly control number and energy of protons collectively accelerated as different bunches. *Nucl. Instrum. Methods Phys. Res. A* **2021**, *998*, 165190. [[CrossRef](#)]
22. Ryzhkov, V.A.; Remnev, G.E.; Pyatkov, I.N.; Zhuravlev, M.V. Contribution of Residual Atmosphere Gases to the Flux of Collectively Accelerated Protons in a Luce Diode. *Tech. Phys. Lett.* **2020**, *46*, 361–363. [[CrossRef](#)]
23. Ryzhkov, V.A.; Remnev, G.E.; Pyatkov, I.N.; Zhuravlev, M.V. Effect of the residual atmosphere pressure on collective acceleration of ions in the Luce diode. *Vacuum* **2021**, *187*, 110081. [[CrossRef](#)]
24. Kurkin, S.A.; Koronovskiy, A.A.; Khramov, A.E. Specific features of virtual cathode formation and dynamics with allowance for the magnetic self-fields of a relativistic electron beam. *Plasma Phys. Rep.* **2013**, *39*, 296–306. [[CrossRef](#)]

Disclaimer/Publisher's Note: The statements, opinions and data contained in all publications are solely those of the individual author(s) and contributor(s) and not of MDPI and/or the editor(s). MDPI and/or the editor(s) disclaim responsibility for any injury to people or property resulting from any ideas, methods, instructions or products referred to in the content.